(n=6). Machining each coping required eight hours. Y-TZP copings were machined in 100-μm increments, as measured using calipers integrated into the laser machine for depth control. At first machining, the machining residue in the width direction of Y-TZP coping occurred on the inner surface so that the convergence angle of coping was greater than 11°, as designed based on machining 3D-CAD data. Therefore, the coping was machined two, three, or four times until the machining residue disappeared (Fig. 3).

Machining accuracy

1. Evaluation of machining accuracy by 3D measurement

Machined Y-TZP copings were measured using a non-destructive industrial 3D scanner (ATOS I 2M, GOM mbH, Brunswick, Germany) at every machining, and 3D-CAD data of copings were constructed. Dimensional differences in the height direction and width direction between the 3D-CAD data for machined Y-TZP copings and the target 3D-CAD data of Y-TZP copings were inspected using inspection software (GOM inspect, GOM mbH, Brunswick, Germany). Twelve measurement points were set in the width direction: 0, 0.5, 1, 1.5, 2, 2.5, 3, 3.5, 4, 4.5, 5, and 5.5 mm away from the inner cervical line of the Y-TZP coping (Fig. 4). In the height direction, six measurement points were set: −3, −2, −1, 0, 1, 2, and 3 mm away from the occlusal center of Y-TZP coping (Fig. 4). The results for the dimensional differences in the width direction and the machining frequency were analyzed by two-way repeated-measures ANOVA and Sidak's multiple comparison test. One-way repeated-measures ANOVA and Sidak's multiple comparison test were used to analyze the results for the dimensional differences in the height direction. The convergence angle of the inner coping was measured at each machining. One-way repeated measures ANOVA and Sidak's multiple comparison test were used for analyzing the results of the convergence angle of inner-machined copings.

2. Evaluation of machining accuracy using metal dies

Machined copings at the fourth machining were measured using dies having different cervical widths of 9.60 mm (Abutment 1), 9.58 mm (Abutment 2), and 9.56 mm (Abutment 3). The convergence angle of each die was 11°. Y-TZP copings were placed on the metal die (Fig. 5) without cementation, and the marginal discrepancy (L-L1) was measured using a measuring microscope (STM6, OLYMPUS, Tokyo, Japan). Negative values for L-L1 indicate that copings were machined smaller than the machining CAD, whereas positive numbers indicate that the copings were machined larger than the machining CAD (Fig. 5). One-way ANOVA and Sidak's multiple comparison test were used to analyze the results for the goodness of fit.

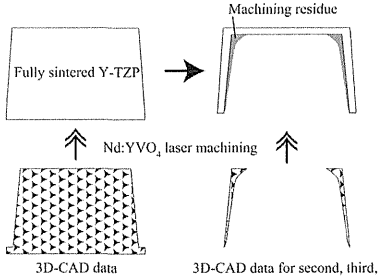

Fig. 3 Method of fabricating a zirconia coping having an inner taper of 11° and a cervical width of 9.6 mm.

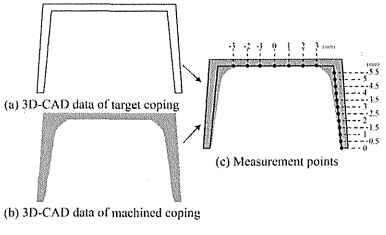

Fig. 4 Schematic diagrams of 3D measurement for machining accuracy.
The dimensional differences between (a) and (b) were inspected using inspection software. (c) Measurement points in the height and width directions.

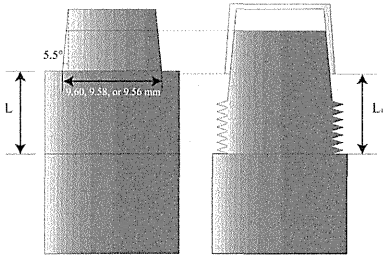

Fig. 5 Schematic diagrams of a metal die having a taper of 11° used to evaluate machining accuracy.

RESULTS

Determination of the most appropriate power level of the Nd:YVO$_4$ laser

The means and standard deviations (SD) of the calculated average roughnesses (Ra) and the machining depths of the irradiated Y-TZP surfaces are shown in Table 2 and Fig. 6.

The values of Ra for average powers of 6 W, 7.5 W, and 9 W were smaller than those for average powers of 3 W and 12 W, and the values of Ra for average powers of 6 W and 7.5 W were smaller than that for an average power of 14 W ($p<0.05$). Therefore, the Y-TZP surface was machined to be the smoothest at 6 W and 7.5 W using the Nd:YVO$_4$ laser. As the average power increased, the machining depth tended to increase, but became smaller from 12 W to 14 W. The machining depths per pulse for average powers of 7.5 W, 9 W, 12 W, and 14 W were greater than that for an average power of 3 W ($p<0.05$), and machining depth per pulse for an average power of 12 W was greater than that for an average power of 6 W ($p<0.05$). When the above analysis results for the calculated average roughness and the machining depth were put together, the average power level of 7.5 W, at which the smoothest Y-TZP surface could be obtained with high machining efficiency, was decided to be the most appropriate power level.

Table 2 Average roughness and machining depth per pulse after nanosecond laser irradiation of fully sintered Y-TZP

Average power (W)	Average roughness (Ra, μm)	Machining depth (μm)
	Mean (SD)	Mean (SD)
3	0.63 (0.11)	1.9 (1.4)
6	0.37 (0.06)	3.7 (0.4)
7.5	0.40 (0.05)	4.8 (0.5)
9	0.43 (0.02)	5.5 (0.6)
12	0.67 (0.07)	5.9 (0.6)
14	0.62 (0.07)	4.7 (0.2)

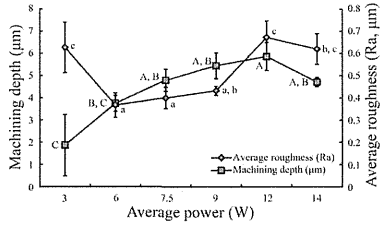

Fig. 6 Means and standard deviations of calculated average roughnesses (Ra) and machining depths of irradiated Y-TZP surfaces for different average power levels.
The six average power levels were statistically divided into three subgroups (a, b, and c) with respect to average roughness and three subgroups (A, B, and C) with respect to machining depth. Means with different letters are significantly different ($p<0.05$).

Machining Y-TZP copings using the Nd:YVO$_4$ laser machine

An optimal machining condition with an average power of 7.5 W was used to machine Y-TZP copings from fully sintered specimens. At first machining, machining residue was deposited in the width direction on the inner surface of the Y-TZP copings, so that the convergence angle was greater than 11°, which were designed as the machining 3D-CAD data (Fig. 3). The machining residue of Y-TZP copings was measured using an industrial 3D scanner, and the machining data were reacquired. The Y-TZP copings were then machined again using the new data. This process was repeated for the same Y-TZP coping until the fourth machining.

Machining accuracy

1) Machining accuracy using 3D measurement

Figure 7 and Table 3 show the dimensional difference in the height direction for a certain section between the CAD data of the machined Y-TZP copings and the target CAD data for the coping obtained through 3D measurement. The average dimensional difference in the height direction was 73.6 μm. Figure 8 and Table 4 show the dimensional difference in the width direction obtained using 3D measurement. Two-way repeated-

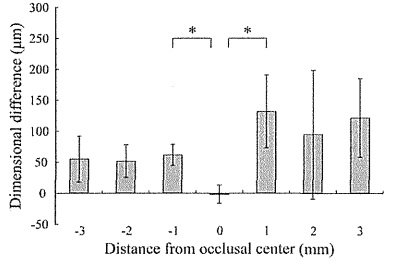

Fig. 7 Means and standard deviations of dimensional differences in the height direction.
The asterisk (*) indicates a significant difference at $p<0.05$.

Table 3 Dimensional difference in the height direction at each measurement point

Distance from occlusa center (mm)	Dimensional difference (μm)	
	Mean	(SD)
−3.0	55.0	(37.3)
−2.0	51.7	(26.4)
−1.0	61.7	(17.2)
0.0	−1.7	(14.7)
1.0	131.7	(58.8)
2.0	95.0	(130.9)
3.0	121.7	(63.7)

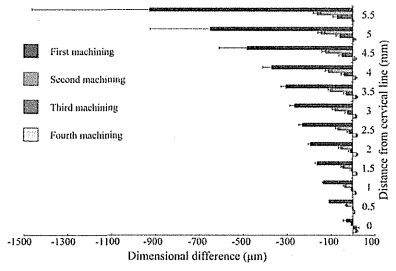

Fig. 8 Means and standard deviations of dimensional differences in the width direction.

measures ANOVA revealed that both main effects were significant ($p<0.01$). As shown in Fig. 8, the dimensional difference in the width direction decreased as the number of machining iterations increased and as the distance from the cervical line decreased, although the interaction between the two primary effects was also significant ($p<0.05$). The simple primary effect of the distance from the cervical line was not significant at the third or fourth machining ($p<0.05$). The dimensional difference in the width direction at the fourth machining was at most approximately 20 μm.

Figure 9 shows the inner convergence angle of machined copings of particular cross sections. The means and standard deviations, which are shown in parentheses, of the inner surface convergence angle were

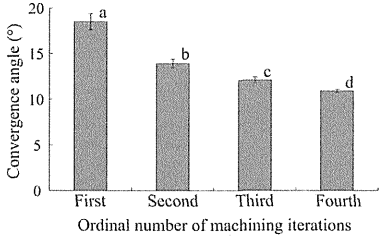

Fig. 9 Means and standard deviations of convergence angles of inner machined copings. Means labeled with different letters (a, b, c, and d) are statistically different from each other ($p<0.01$).

Table 4 Dimensional difference in the width direction at each measurement point

Distance from cervical line (mm)	Dimensional difference (μm)							
	First machining		Second machining		Third machining		Fourth machining	
0.0	−30.1	(14.8)	−6.5	(3.0)	15.1	(12.0)	17.2	(5.0)
0.5	−107.5	(2.9)	−31.0	(4.7)	−1.9	(3.0)	7.6	(0.6)
1.0	−132.6	(4.6)	−36.3	(6.1)	−3.1	(4.4)	14.0	(2.8)
1.5	−161.9	(9.0)	−44.7	(8.3)	−6.0	(5.5)	18.2	(2.7)
2.0	−192.2	(10.9)	−55.3	(9.3)	−10.8	(8.0)	20.0	(2.4)
2.5	−229.2	(16.3)	−68.0	(10.4)	−16.7	(8.7)	19.1	(3.9)
3.0	−265.0	(21.4)	−81.1	(12.7)	−23.5	(12.0)	16.5	(4.2)
3.5	−305.6	(21.8)	−102.6	(10.3)	−30.0	(12.2)	17.8	(4.5)
4.0	−369.4	(40.1)	−110.6	(15.7)	−39.0	(14.1)	14.3	(5.8)
4.5	−481.8	(127.6)	−125.0	(16.4)	−48.2	(15.8)	11.5	(5.7)
5.0	−649.0	(274.6)	−143.9	(16.8)	−58.2	(19.4)	6.8	(6.9)
5.5	−926.4	(536.0)	−162.8	(17.9)	−70.6	(20.5)	1.8	(5.1)

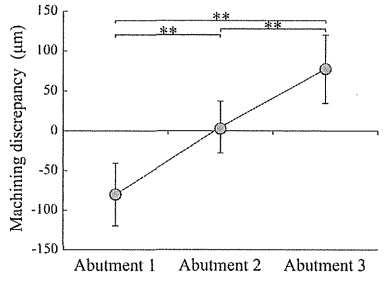

Fig. 10 Machining accuracy using three metal dies having convergence angles of 11° and different cervical widths; Abutment 1: 9.60 mm, Abutment 2: 9.58 mm, and Abutment 3: 9.56 mm. Significant differences are indicated by asterisks '**' ($p<0.01$).

determined to be as follows: 18.5° (0.86°) for the first machining, 13.9° (0.47°) for the second machining, 12.1° (0.34°) for the third machining, and 10.9° (0.18°) for the fourth machining. One-way repeated-measures ANOVA revealed that the number of machinings significantly affected the inner convergence angle of Y-TZP coping. As the number of machining iterations increased, the convergence angle decreased significantly ($p<0.01$). At the fourth machining, the convergence angle was comparable to the target 3D-CAD data.

2) Machining accuracy using the metal dies

The marginal fits of the Y-TZP copings that were machined four times were measured using metal dies. The means and standard deviations, which are shown in parentheses, of L-L1 were −80.2 (40.0) μm, 4.8 (32.6) μm, and 77.0 (42.0) μm using Abutments 1, 2, and 3, respectively. The larger the cervical width, the smaller the value of L-L1 (Fig. 10). The copings fit accurately on Abutment 2.

DISCUSSION

Determination of the most appropriate power level of the Nd:YVO_4 laser

The average roughness and machining depth were measured in order to determine the most appropriate average power level (W) of the Nd:YVO_4 laser on fully sintered Y-TZP. Excellent lasing performance on Y-TZP, which has high machining efficiency and provides a smooth surface, is most important. As shown in Fig. 6, the six average power levels considered herein were statistically divided into three subgroups (a, b, and c) with respect to average roughness and three subgroups (A, B, and C) with respect to machining depth. The average power level of 7.5 W belonged to both subgroup a (smallest average roughness) and subgroup A (greatest machining depth). Therefore, the average power level of 7.5 W, at which the smoothest Y-TZP surface could be obtained with high machining efficiency, was considered to be the most appropriate power level for the Nd:YVO_4 laser. High machining efficiency reduces the machining time.

Machining accuracy of Y-TZP copings

The copings, which were extracoronal restorations, were able to be machined from fully sintered Y-TZP using the nanosecond laser. Figure 7 shows that the dimensional difference in the height direction was not uniform. Air was blown from three directions on the Y-TZP coping in order to avoid reattachment of fine particles. However, locational differences were thought to occur as a result of the air being blown non-uniformly against the copings. Controlling the depth direction in machining (Z-axis) using a focused laser beam is generally difficult. Therefore, the copings were machined using an improved method for the depth control. In this experiment, the dimensional difference in the height direction was at most 132 μm for the planned 6.5 mm in the height direction based on machining CAD data, which gives an error of only 2.0%. In the width direction, the dimensional difference was at most 20 μm. The mean and standard deviation of the convergence angles of the inner copings were 10.9° and 0.18°, respectively.

In addition, the inside of the coping might be slightly oval-shaped. Therefore, in order to clinically evaluate the precision, a traditional experiment was conducted in which the dimensional accuracy was evaluated using a die method. We prepared three metal dies having different cervical widths. Since the machining 3D-CAD data (Fig. 2) did not take into account the cement layer or the coefficient of friction, the marginal discrepancy at the cervical line could not be obtained using Abutment 1, the cervical width of which was the same as in the machining 3D-CAD data. Therefore, dies having smaller cervical widths had to be used to measure the marginal discrepancy. The results revealed that the copings fit accurately on the die. The aforementioned discrepancies could be further improved by a slight modification of the design program of the CAD system. Marginal discrepancies of less than 120 μm have been reported to be clinically acceptable[9]. Thus, accurate machining of zirconia coping for clinical use using the Nd:YVO_4 laser is possible.

Laser machining of Y-TZP

At present, Y-TZP copings are fabricated using a dental CAD/CAM system in which a partially sintered Y-TZP block (12 HV) is milled and subsequently sintered in a furnace. Machining design can compensate for the approximately 20% volume shrinkage that occurs later during sintering of the zirconia blocks. Therefore, we devised a new method by which to machine a Y-TZP coping directly from a fully sintered Y-TZP block using an industrial Nd:YVO_4 Q-switched nanosecond

laser. The use of lasers to machine ceramics presents a number of advantages over the other methods. Laser machining is a noncontact technique that allows high-precision machining of numerous types of ceramics and eliminates tooling costs, which are expensive.

Generally, the material properties of Y-TZP, specifically its high thermal expansion coefficient (11×10^{-6}/°C) and low thermal conductivity (2 W/mK)[10], make laser machining of this material difficult. Due to the strong thermal nature of the laser beam-material interaction, especially in the case of long pulse widths, microcracks are generated by dental lasers, which generate millisecond-order pulse widths, as a result of thermal damage. In the present study, we used a nanosecond pulsed laser, which could significantly reduce thermal damage. The formation of cracks in the irradiated surface was seldom observed when using the nanosecond laser, and cracks that observed were extremely small, having depths of approximately 3 μm. Thus, the use of an ultrashort pulse laser that produces a picosecond pulsed laser or a femtosecond pulsed laser can significantly reduce the above-mentioned thermal effects, such as thermal damage or microcracks. However, such lasers require too much machining time to be adapted for practical application. Therefore, the potential of nanosecond laser machining on Y-TZP was demonstrated herein. Approximately 90% of the material removed through the proposed laser machining is a result of the interaction between the laser beam and the surface of the Y-TZP workpiece being machined. The nanosecond laser used is thus suitable for use in the machining of dental restorations.

The laser machine used herein provided three-axis machining, in which a Y-TZP specimen was irradiated from one direction (Z-axis). In addition, machining a hole with a convergence angle by condensing a laser beam has certain limitations because a focused laser produces a tapered hole. Accurately machined copings for clinical use were obtained after the fourth machining. On the other hand, a five-axis laser machine can instantly machine a taper-less hole because the laser beam can irradiate vertically with respect to the work piece[11]. In other words, a five-axis machine would provide the Y-TZP copings with improved retention and accuracy for clinical use and reduce costs by reducing the machining and finishing times.

Figure 11 shows a crown coping that was machined at an average power of 7.5 W. A dental restoration more complicated than the simple abutment coping shown in Fig. 2 was successfully machined from a fully sintered Y-TZP block, as shown in Fig. 11.

In comparison with a Nd:YAG laser, the Nd:YVO_4 laser has advantages such as the ability to produce more compact systems, because the Nd:YVO_4 crystal has 5 times higher absorption coefficient than Nd:YAG crystal. In addition to this, the laser has a higher efficiency thanks to a high stimulated emission cross section. A Nd:YVO_4 single crystal can be used for compact, high-efficiency machining, as compared with a Nd:YAG single crystal[12,13].

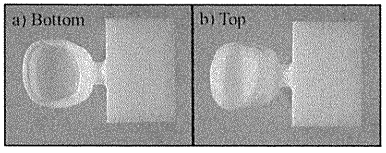

Fig. 11 A crown coping machined at an average power of 7.5 W.
The crown coping was successfully fabricated in a clinical form.

Darkening of the machined Y-TZP surface and corresponding countermeasures

After ultrasonic cleaning, the machined Y-TZP surface was dark gray. Darkening of Y-TZP irradiated by a nanosecond laser should be a result of oxygen vacancies that were generated at high temperatures due to the release of oxygen atoms after substoichiometric dioxide formation, in which ZrO_2 became ZrO_{2-X}[14,15]. Noda *et al.* reported that a surface irradiated by a Nd:YAG laser became darkened and that the oxygen concentration clearly decreased, whereas the zirconium concentration increased[7]. Irradiated Y-TZP disks heated at 1,000°C for 5 min in air retuned to their original white color. Applying the above reduction reaction to the present study, Y-TZP was heated in the atmosphere to reabsorb oxygen. After heating, the Y-TZP became white again. The high temperature allows oxygen to diffuse back to vacancies in the irradiated surface, rebuilding the crystalline structure and recovering the white color of Y-TZP. This heating is thought not to have an adverse clinical effect because the porcelain is sintered on Y-TZP at higher than 1,000°C. Matysiak *et al.* reported a similar result in which blackening occurred within holes on zirconia irradiated using a HeNe laser[16]. After heating at 1,350°C, the sample became white again, and there was no significant variation after the heat treatment. The recovery of the white color of the surface enables the fabrication of esthetic dental prostheses without opaquing using Y-TZP machined with a Nd:YVO_4 laser. The effect of the nanosecond laser on the machined Y-TZP surface was small, and we assume that the mechanical properties will not be adversely affected to a significant degree.

Future development

The primary problems associated with the laser machining of Y-TZP reported herein are a long machining time and high cost. Fabrication of the inner surface of the Y-TZP coping required approximately eight hours. However, sintering a partially sintered zirconia coping fabricated by a CAD/CAM system requires up to 18 h. Moreover, the long machining time required when using the laser can be shortened by using a prefabricated coping of fully sintered Y-TZP.

A nanosecond laser machine that can machine a high-thermal-expansion, low-thermal-conductivity material, such as Y-TZP, will also be able to machine other dental materials, such as resins and metals. If the machine is miniaturized and becomes widely used, the cost may be reduced considerably.

The toughness and high strength of Y-TZP are similar to the characteristics of metallic materials. For this reason, Y-TZP has been used in numerous applications in which previously only metals were believed to be suitable, such as moving parts of engines, valve components, milling and cutting tools, wire-drawing dies, and scissors[8]. Y-TZP is also a popular material for use in bio-medical applications due to its outstanding mechanical properties, reliability, and excellent biocompatibility. The ability to carry out accurate laser machining of Y-TZP would allow its properties to be more widely exploited, in particular for applications in which uniquely shaped, intricately structured components are required, not only in industry but also in dentistry.

CONCLUSIONS

A Y-TZP coping was fabricated using a CAD/CAM system in which a partially sintered Y-TZP block was milled and subsequently sintered in a furnace, because fully sintered Y-TZP is too difficult to machine using milling techniques. Furthermore, the design compensates for the volume shrinkage that occurs during sintering of Y-TZP blocks. Thus, we devised a new method by which to machine Y-TZP copings using an industrial Nd:YVO_4 Q-switched nanosecond laser. The following conclusions were obtained based on the results of the present study.

1. An average power of 7.5 W was determined to be the optimal lasing condition because this condition provided the smoothest surface with high machining efficiency.
2. The convergence angle of the inner coping obtained at the first machining did not adequately agree with the provided machining 3D-CAD data. At the fourth machining, however, the convergence angle of the inner coping was 10.9° (SD=0.18°), which is approximately the same as the provided machining 3D-CAD data.
3. The dimensional difference in the height direction was at most 132 μm (SD=59 μm), and the dimensional difference in the width direction at the fourth machining was at most 20 μm (SD=2.4 μm).
4. The machined copings fit accurately on the metal die.
5. The proposed method using a nanosecond Nd:YVO_4 laser machine was demonstrated to be useful for fabricating a coping directly from fully sintered Y-TZP.

REFERENCES

1) Rosenstiel SF, Land MF, Fujimoto J. Contemporary fixed prosthodontics. 3rd ed. St. Louis: Mosby; 2001: p.262-271.
2) Conrad HJ, Seong WJ, Pesun IJ. Current ceramic materials and systems with clinical recommendations: A systematic review. J Prosthet Dent 2007; 98: 389-404.
3) Sjogren G, Lantto R, Granberg A, Sundstrom BO, Tillberg A. Clinical examination of leucite-reinforced glass-ceramic crowns (Empress) in general practice: a retrospective study. Int J Prosthodont 1999; 12:122-128.
4) Beuera F, Aggstaller H, Edelhoff D, Gernet W, Sorensen J. Marginal and internal fits of fixed dental prostheses zirconia retainers. Dent Mater 2009; 25: 94-102.
5) Denry I, Holloway JA. Ceramics for dental applications: A review. Materials 2010; 3: 351-368.
6) Yamagishi T, Ito M, Fujimura Y. Mechanical properties of laser welds of titanium in dentistry by pulsed Nd:YAG laser apparatus. J Prosthet Dent 1993; 70: 264-273.
7) Noda M, Okuda Y, Tsuruki J, Minesaki Y, Takenouchi Y, Ban S. Surface damages of zirconia by Nd:YAG dental laser irradiation. Dent Mater J 2010; 29: 536-541.
8) Wang X, Shephard JD, Dear FC, Hand DP. Optimized nanosecond pulsed laser micromachining of Y-TZP ceramics. J Am Ceram Soc 2008; 91: 391-397.
9) McLean JW, von Fraunhofer JA. The estimation of cement film thickness by an in vivo technique. Br Dent J 1971; 131: 107-111.
10) Vagkopoulou T, Koutayas SO, Koidis P, Strub JR. Zirconia in dentistry: Part 1. Discovering the nature of an upcoming bioceramic. Eur J Esthet Dent 2009; 4: 130-151.
11) Erkorkmaza K, Alzaydia A, Elfizyb A, Enginb S. Time-optimal trajectory generation for 5-axis on-the-fly laser drilling. CIRP ANN 2011; 60: 411-414.
12) Campanelli SL, Casalino G, Ludovico AD, Bonserio C. An artificial neural network approach for the control of the laser milling process. Int J Adv Manuf Technol 2013; 66: 1777-1784.
13) Friel GJ, Conroy RS, Kemp AJ, Sinclair BD, Ley JM. Q-switching of a diode-pumped Nd:YVO_4 laser using a quadrupole electro-optic deflector. Appl Phys B 1998; 67: 267-270.
14) Yoshioka S, Kobayashi T, Tanaka Y, Yamamoto Y, Miyazaki T. Blackening and crack formation in Q-switched YAG laser machining of zirconia ceramics. J Jpn Soc Prec Eng 1989; 55: 1277-1282.
15) Janek J, Korte C. Electrochemical blackening of yttria-stabilized zirconia–morphological instability of the moving reaction front. Solid State Ionics 1999; 116: 181-195.
16) Matysiak M, Parry JP, Crowder JG, Hand DP, Shephard JD, Jones N, Jonas K, Weston N. Development of optical techniques for noncontact inspection of Y-TZP parts. Int J Appl Ceram Technol 2011; 8: 140-151.

Ⅲ．研究成果の刊行に関する資料⑦

J. Electr. Electron Syst., 3:118 (2014)

Electrical & Electronic Systems

Kameda and Ohkuma, J Electr Electron Syst 2014, 3:1
http://dx.doi.org/10.4172/2332-0796.1000118

Review Article Open Access

Electromagnetic Fields from Dental Devices and their Effects on Human Health

Takashi Kameda[1]* and Kazuo Ohkuma[2]

[1]Department of Orthodontics, Nippon Dental University, Niigata, Japan
[2]Department of Dental Materials Science, Nippon Dental University, Niigata, Japan

Abstract

Magnetic fields can cause human health problems. Low-frequency electromagnetic fields are sometimes induced by electric currents in metallic objects that are worn or used in or on the body, and are unlike the high-frequency electromagnetic fields that produce heat. In low-frequency magnetic fields, the strength of the induced electric current is believed to be more important than the magnetic field strength in terms of effects on the health of living bodies. Electrically powered dental devices, including personal devices such as electric toothbrushes and professional devices such as curing lights for light-cured dental resins, are widely used because of their convenience, but the electric circuits and motors that power them produce low-frequency electromagnetic waves. These magnetic fields induce electric currents in teeth and in metallic appliances that are set in the oral cavity. The effects of these induced currents on human health must therefore be considered. Investigations of this issue revealed that magnetic fields from dental devices promoted the corrosion of intraoral metallic appliances via the induced currents, and this is likely to cause metallic allergies. Almost all reports on the effects of magnetic field exposure, including this corrosion phenomenon, describe harmful effects on human health. However, there may be some effective uses of the magnetic fields generated by dental devices for human health promotion. Oral bacteria were found to corrode orthodontic stainless steel appliances, but magnetic field-induced currents in these appliances could provide remarkable protection effects against this microbially induced corrosion. In this review, we discuss the results and conclusions of these investigations especially about novel ways of harmful effects and effective use of magnetic fields from dental devices, and conclude that further detailed studies are required to clarify their detailed mechanisms and to develop countermeasures for protection from or effective use of these fields.

Keywords: Low frequency; Induced current; Corrosion; Electric toothbrushes; Curing lights; Dental appliances; Tooth; Microbiologically influenced corrosion; Protection against corrosion

Introduction

There has been considerable recent interest in the effects of electromagnetic fields (such as those near electricity transmission lines) on human health, and particularly in their potential to effect the development of leukemia and central nervous system tumors. An elevated risk of leukemia following exposure to electromagnetic fields has been demonstrated [1,2], and the International Agency for Research on Cancer (IARC), the International Commission on Non-Ionizing Radiation Protection (ICNIRP) and the World Health Organization (WHO) have each established guidelines and criteria to outline the roles and risks of magnetic fields (MFs) in carcinogenesis [3-5]. However, other reports in the literature have found no significant correlation between exposure to electromagnetic fields and leukemia [6,7]. The results from studies of the correlation between electromagnetic field exposure and the risks of central nervous system tumors are also inconclusive [2,7]. These findings with regard to the risks of electromagnetic fields inducing leukemia or central nervous system tumors should be considered in terms of dependence on the electromagnetic field exposure conditions, such as field intensity and exposure time [8,9].

Many home electrical appliances, including personal dental devices, generate MFs [10,11]. In the dental field, the effects of MFs on human health are thought to be more serious when compared with many other medical fields, because the MF-generating devices are used near the craniocervical area. In a study of dental clinics, electromagnetic fields were detected, and each professional dental device that was set up in the clinics was reported to generate MFs [12]. However, exposure to MFs from professional dental devices for use in dental clinics might be considered to have little effect on the patients, because of the limited times and numbers of clinic visits for each patient. In a questionnaire-based survey of the tooth brushing habits of 1200 Japanese people (600 males and 600 females, with an age range from teens to sixties), 52.5% of the respondents cleaned their teeth twice a day, and 48% had brushing times of 1–3 min [13]. Based on these figures, the average Japanese person's brushing time was estimated to be 120 min/month (2 min × 2 times/day × 30 days), and 1440 min/year. For these reasons, we focused on personal dental devices, and on electric toothbrushes in particular, as the main MF sources. The effects of MF exposure from electric toothbrushes on user health are likely to slowly but surely increase.

In this review, we describe the effects of MFs from electric toothbrushes and other dental devices on dental appliances and teeth that could affect human health. In addition, interesting unpublished data and speculation with regard to MF effects are given in this paper.

MFs from Dental Devices

Electric toothbrushes are widely used because of their convenience. However, they have also been reported to produce low-frequency electromagnetic fields, which could cause health problems, e.g. interference with pacemakers [10,14]. In dental clinics, light-cured resins that are polymerized by curing light sources, which have also been reported to produce low-frequency electromagnetic fields, are also widely used for both convenience and speed [11].

The MFs produced by dental devices, e.g. by electric toothbrushes and curing light sources for light-cured resin, and their frequencies were evaluated. We estimated MFs within the 1–2000 Hz frequency range, in keeping with our preliminary study and with the previous literature, which indicated that this was the appropriate range to monitor [10,15]. Five commercially available electric toothbrushes and three commercially available curing lights that were investigated generated MFs [16]. The MFs produced by each representative dental device are shown in Figure 1. The MFs produced by each of the electric toothbrushes were found to be at quite different levels [16]. These MF levels could reflect the cleaning ability of each electric toothbrush. Further investigation of the relationship between MF level and cleaning ability is necessary, and should be useful as part of a design and construction strategy for the development of electric toothbrushes with low MFs and high cleaning ability. Interestingly, the MF levels from curing lights were found to be at low levels in Light-Emitting Diode (LED)-type lights and at high levels in halogen-type lights [17]. Compared with LED-type curing lights, halogen-type curing lights generated much more heat. To prevent these curing lights from overheating, cooling fans with electric motors were built into the halogen-type curing lights. The MF levels of these lights were believed to be dependent on the strengths of the fan electric motors. Similarly, the MFs from electric toothbrushes were found to be at different levels at the front, back, right and left sides of the brushes, which is likely to be related to the location of the motor or other electrical components inside the toothbrushes.

MFs from Dental Devices Induce Electric Currents in Intraoral Metallic Appliances and Teeth

Many questions have been raised with regard to the effects of MFs from dental devices on human health. There are questions over whether or not these effects are harmful or harmless, and over the mechanisms of MF effects on human health. Many home electrical appliances and professional dental devices generate low-frequency MFs that can induce electric currents in the human body and within any metallic objects or devices worn in or on the body [10,15]. In low-frequency MFs, the strength of the induced electric current is thought to be more important than the strength of the MF itself in terms of the effects on the health of living bodies [18]. To create a framework to discuss these questions, we set up our hypothesis as follows. (1) Dental electrical devices generate MFs (as already described in the previous section) [16,17]. (2) These MFs can induce electric currents in teeth and metallic appliances that are set in the oral cavity [17]. (3) The induced currents produce certain effects that may have an influence on human health. Initially, we investigated part 2 of the hypothesis, e.g. that currents are induced in metallic appliances and teeth by MFs from dental devices (Figure 2). MF exposure was found to induce electric currents in every dental metallic appliance, which were made of various metals, including stainless steel (SUS), CoCr, 70%Ag alloy, 12%Au-40%Ag-20%Pd alloy, nickel titanium, β-titanium (Ti-11.5MO-6Zr-4.5Sn) and pure titanium [16]. Interestingly, the measured electric voltages and currents that were induced in the dental appliances were not dependent on the electrical resistivity values of the materials, but on their shapes and specific metal contents [16].

Electric currents were also induced in human hard tissues such as tooth and bone by MFs, and the roles that they play in the living body must be considered, because they may simply cause pain, or may perform roles in bone formation and repair similar to the methods based on electrical or electromagnetic field stimulation (which use MF-induced currents) [19,20]. To clarify these roles, currents induced in teeth by MFs from electric toothbrushes and curing lights were investigated. Induced currents were observed in teeth under MF exposure. We found that the voltages induced in teeth by electric toothbrushes were higher (10^2–10^3 μV) than those previously measured in dental appliances (10^1–10^2 μV) [16,17]. In contrast, the currents induced by electrictoothbrushes in

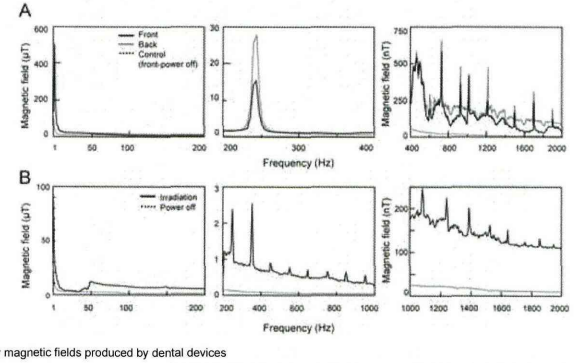

Figure 1: Low-frequency magnetic fields produced by dental devices

A: electric toothbrush (Philips Sonicare HX9100, Philips Oral Healthcare Inc., Bothell, WA); B: curing light (OPTILUX500, Kerr Inc., Camano Island, WA). The MFs produced by the electric toothbrushes and the curing lights, and their frequencies were detected and evaluated using a spectrum analyzer (SPECTRAN NF-5035, Aaronia AB Inc., Euscheid, Germany). The MFs were estimated at 2 cm distances from the front and back sides of activated or inactive electric toothbrushes, and 1 cm distances from the light guide tips of activated or inactive curing lights.

***Corresponding author:** Takashi Kameda, Department of Orthodontics, Nippon Dental University, School of Life Dentistry at Niigata, 1-8 Hamaura-cho, Chuo-ku, Niigata 951-8580, Japan, Tel: +81-25-267-1500 ext. 3303; Fax: +81-25-267-1622; E-mail: tkameda@ngt.ndu.ac.jp

Received December 19, 2013; **Accepted** January 06, 2014; **Published** January 08, 2014

Citation: Kameda T, Ohkuma K (2014) Electromagnetic Fields from Dental Devices and their Effects on Human Health. J Electr Electron Syst 3: 118. doi:10.4172/2332-0796.1000118

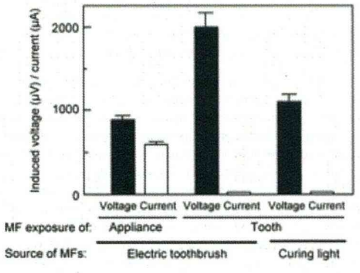

Figure 2: Electric voltages and currents induced in SUS multibracket system and tooth by dental devices at a distance of 1 cm between device and appliances.

Appliance: multibracket system consisting of brackets (SUS304 × 10, SuperMesh Bracket, Tomy International Inc., Tokyo, Japan), molar tubes (SUS304 × 2, Single Tube, Tomy International Inc.), molar bands (SUS304 × 2, Ideal Molar Band, Tomy International Inc.), and wire (SUS304 × 1, Suzuki stainless steel wire, Mitsuba Ortho Supply Inc., Tokyo, Japan). Tooth: human maxillary premolar tooth of patient undergoing orthodontic treatment. Electric toothbrush: Philips Sonicare HX9100. Curing light: OPTILUX500. The electric currents induced in dental devices were estimated using a digital multimeter (7351 A/E, ADC Corporation, Tokyo, Japan) in AC+DC mode (i.e. voltage=$(ACV^2+DCV2)^{1/2}$, and current=$(ACI^2+DCI2)^{1/2}$).

	Bracket + wire		Bracket only	
	MF (−)	MF (+)	MF (−)	MF (+)
Cr	–	+	–	–
Fe	0.20±0.012	1.39±0.067*	0.11±0.018	0.71±0.082*
Ni	–	+	–	+
Sn	na	na	–	–
Ti	na	na	–	–

n=6 for each experimental condition. SUS: stainless steel wire; MF: magnetic field; +: detected values (3.3δ/slope) ≤ values < determination limit (10×$2^{1/2}$δ/slope); –: values <detection limit; and na: not available. The data were analyzed via the Mann-Whitney U test to define the statistically significant differences. Superscript asterisks denote the statistically significant differences ($p<0.05$) within each appliance compared with *MF(−).

Table 1: Elution amount of each element (μg) from SUS appliances to artificial saliva.

teeth were lower (≈10^1 μA) than those previously measured in dental appliances (10^1–10^3 μA) [16]. This difference could relate to disparities between the electrical resistivities of tooth tissue (≈10^3 Ω m) and metals (e.g. stainless steel ≈ 10^{-8} Ω m) [21,22]. We predicted that the ranking order in which currents could be induced in different bracket materials with completely same bracket shape and size (KBT metal bracket; SUS304, KBT zirconia bracket; ZrO_2, Rocky Mountain Morita Inc., Tokyo, Japan) would be tooth+stainless steel bracket > tooth+zirconia bracket ≈ tooth, based on their electrical resistivities (tooth, 10^3 Ω m; stainless steel, 10^{-8} Ω m; ZrO_2, 10^{10}–10^{12} Ω cm; resin (acrylic), 10^{13}–10^{14} Ω m) [23,24]. However, we found that the actual ranking order was tooth+zirconia bracket > tooth+stainless steel bracket > tooth [17]. The reason for this unexpected result is unclear. The presence of the adhesive does not appear to be a factor, because the induced currents with and without adhesive (no bracket) were comparable. The resistivity of the bracket material also appears to be insignificant, because the induced current was greater in teeth that were attached to ZrO_2 or stainless steel brackets than in teeth that were bonded to identically shaped acrylic brackets (unpublished data). Despite considerable efforts, we have been unable to correlate these results with any specific material property. It is likely that this unexpected induced current ranking order is because of a combination of tooth properties and the material properties of the appliance components rather than the materials and their resistivities alone.

In any case, MFs from personal and professional dental devices induced currents, not only in the metallic dental appliances, but also in teeth. The effects of these induced currents on human health must now be considered.

MFs from Dental Devices Promote Corrosion of Intraoral Metallic Appliances via Induced Currents

Currents induced in intraoral metallic appliances by MFs from dental devices must have some effects. We must therefore determine these effects.

Previous results showed that the MFs from electric toothbrushes could induce alternating electric currents in both dental metallic appliances and teeth [16,17]. Electric currents in oral appliances, *e.g.* galvanic currents, could cause both discomfort for the user and corrosion of the metallic dental appliances [25,26]. Currents induced by electric toothbrushes were also thought to cause some problems in the oral condition of patients. However, the currents induced by the MFs from dental devices are unlike galvanic currents [16,17]. Galvanic currents, which are direct currents, produced high voltages (several tens to hundreds of mV) with low currents (several tens to hundreds of nA), whereas the electric currents that were induced by electric toothbrushes were of the order of μA to mA with a voltage range of μV to mV [16]. These findings seemed to indicate that galvanic currents were one of the causes of metal corrosion, whereas the electric currents that were induced in dental appliances should not directly cause metal corrosion. However, there were some reports in the literature about metallic corrosion caused by induced Alternating Currents (AC). Rapid geomagnetic variations have been known to induce electric currents in power lines and pipelines, which could then lead to the destruction of power transmission systems and pipeline corrosion [27]. In the stray-current corrosion caused by alternating currents, the induced currents occurred in embedded metal objects lying parallel to the high voltage AC power lines or to the transportation routes of AC electric railways, which then caused the corrosion of the embedded metal objects [28]. Based on these reports, we must therefore consider that the induced currents in metallic appliances produced by MFs from dental devices could be a trigger for corrosion in metallic appliances.

Metallic elution and the surface roughness of metallic appliances immersed in artificial saliva during MF exposure were investigated using a ICP-OES (iCAP 6300 Duo, Thermo Fisher Scientific, Waltham, MA, USA) and a 3D laser confocal microscope (LEXT OLS4000, Olympus Inc., Tokyo, Japan) [29]. MF exposure (120 min; 24 min/day × 5 days) dramatically increased Fe elution, with low levels of Cr and Ni elution from SUS appliances (Table 1). The surface roughness of SUS appliances after MF exposure supported these results (Figures 3 and 4). In contrast to SUS appliances, Ti elution and increased surface roughness were not observed in titanium appliances [29]. In addition, while the induced voltages were almost identical in SUS and titanium appliances, the induced currents in titanium appliances were double those in SUS appliances [29]. These values were not in proportion to the material electrical resistivities, which were 70–80 Ωm for SUS304 and 80–100 Ωm for NiTi. In contrast to the surface roughness evidence

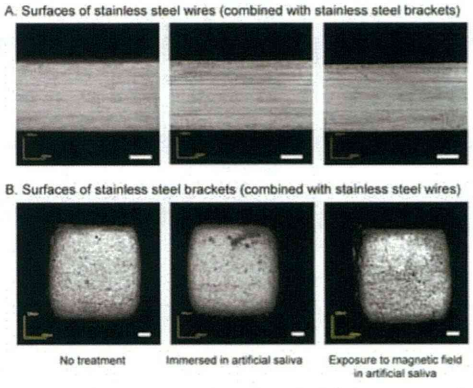

Figure 3: 3D laser confocal micrographs of SUS wire and bracket surfaces immersed in artificial saliva with or without exposure to MFs from electric toothbrushes (×20). The white lines in the micrographs represent 100 μm.

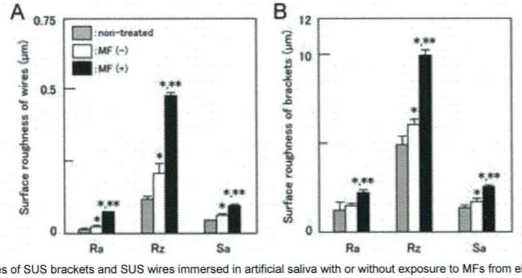

Figure 4: Surface roughnesses of SUS brackets and SUS wires immersed in artificial saliva with or without exposure to MFs from electric toothbrushes.

n=6 for each experimental condition. Ra represents the arithmetic average of the absolute value ($Ra=n^{-1}\Sigma|Yi|$ (i=1-n)), Rz represents the highest peaks and lowest valleys over the entire sampling length, and Sa represents the arithmetic average of the 3D roughness (areal roughness). The data were analyzed via the Mann-Whitney U test to define the statistically significant differences. Asterisks denote the statistically significant differences ($p<0.05$) within each measurement item of each appliance group when compared with *non-treated and **MF(-).

for the occurrence of metallic elution, no pH differences were observed between the non-MF-exposed and MF-exposed groups measured with a pH meter (F-12, Horiba Inc., Kyoto, Japan) [29]. The pH values were lowered by the immersion of the appliance in each case; however, these pH values, which did not reach the depassivation pH, could not have led to the erosion of these alloys [30,31]. However, these pH values in the immersed solutions may not always reflect the local pH values around the appliances.

In any case, these results suggested the following novel MF phenomena for human health. (1) The currents induced in metallic appliances by MFs from dental devices could be one of the causes of SUS corrosion. (2) The corrosion resistivity of titanium alloys is high compared with that of SUS alloys. (3) The pH values of the solutions used for immersion, with or without MF exposure, showed no statistical significance. The low-frequency MFs around the oral cavity that originate from electronic equipment such as electric toothbrushes induce electrical currents in intraorally installed metals (especially in SUS), prostheses and appliances, and promote metallic elution, which is likely to be one of the causes of metallic allergies.

What are the Possible Effects of MFs from Dental Devices on Human Health?

The corrosion of metallic appliances under MF exposure could have detrimental results for human health, such as metal allergies. The induced current itself could also produce similar results, e.g. pain and discomfort for the patients. Because the role of low-

frequency electromagnetic fields in carcinogenesis, and especially in the development of leukemia and central nervous system tumors, has been well-documented [1,2,6-9], the effects of MFs were believed to be basically harmful to human health. It is very difficult to protect ourselves from low-frequency MFs because they can pass through human tissue and most other materials, including glass, plastics, metals and concrete [32]. The only viable way to limit our exposure to low-frequency electromagnetic fields is thought to be to eliminate their generation by electrical home appliances and dental devices.

However, there may also be some effective positive use of MFs generated by dental devices for human health. First, we considered that the induced current in appliances could be used for biocidal applications or for suppression of dental caries- or periodontal disease-causing microorganisms. However, the number of oral bacteria were not reduced, but were actually increased by the electric currents in appliances under MF exposure from dental devices (unpublished data). The oral bacteria suppression effects might not be caused by MF exposure.

The intraoral aging of dental materials includes the plasticization of polymeric adhesives and increased porosity and roughness in metallic alloys, which disturbs the smooth progress in courses of treatment and causes losses in terms of time and money, along with emotional distress for both patients and clinicians [33,34]. The oral environments of living organisms, including those of humans, are most hospitable for biofilm creation and biocorrosion (microbially influenced corrosion or MIC). If MIC existed in oral areas, the currents induced in metallic appliances by MF exposure can be considered a means of protection against corrosion, like electrical protection in other fields. We first investigated the existence of MIC based on oral bacteria. Three representative indigenous oral bacteria, *Streptococcus mutans*, *Streptococcus sanguinis* and *Aggregatibacter actinomycetemcomitans*, were selected for this experiment. *S. mutans* and *S. sanguinis* were oral bacteria that easily created biofilms on the surfaces of the teeth and appliances. *A. actinomycetemcomitans* is a pathogenic bacterium that occurs in localized aggressive periodontitis. We found that *S. mutans* (ATCC49296) and *S. sanguinis* (ATCC25175) corroded SUS dental appliances when the appliances were cultured with them in BHI medium (Brain Heart Infusion medium, Beckton, Dikinson and Company Inc., Detroit, MI, USA) at 37°C in 5 % CO_2 in air in the incubators without shaking from the results of metallic elution and surface roughness of appliances by a ICP-OES and a 3D laser confocal microscope respectively [35], but *A. actinomycetemcomitans* did not corrode SUS or titanium appliances (unpublished data). We then investigated the protection effects of MF-exposure against the biocorrosion of these appliances at a distance of 2 cm between device and appliances. In the groups that were co-cultured with *S. sanguinis*, remarkable protection effects of 120 min (24 min/day × 5 days) - MF exposure against MIC were observed (Figure 5). This MF effect on oral bacterial corrosion of metallic appliances is novel effective use of MFs from dental devices. However, the reasons for this result are unclear, and further detailed investigation is required.

In the orthopedic field, MFs have been used for bone repair in methods based on electrical or electromagnetic field stimulation [19,20]. The MFs from dental devices were found to induce currents in human hard tissue, e.g. teeth [17]. These results indicate the possibility that MFs from dental devices could induce electric currents not only in teeth but also in bone tissue, which would then promote bone formation and repair.

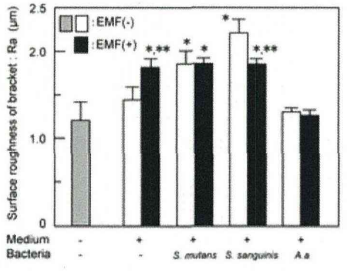

Figure 5: Surface roughnesses of SUS brackets immersed and co-cultured with oral bacteria and with or without exposure to MFs from electric toothbrushes.

n=6 for each experimental condition. Ra represents the arithmetic average of the absolute value. A. a: *Aggregatibacter actinomycetemcomitans*. The data were analyzed via the Mann-Whitney U test to define the statistically significant differences. Asterisks denote the statistically significant differences ($p<0.05$) compared with *intact products (medium (-) and bacteria (-) group) and within each measurement item of each group when compared with **MF(-).

Conclusions and Outlook

This review has discussed the electromagnetic fields of dental devices and their effects on human health. The electromagnetic fields produced by dental devices were basically low-frequency MFs. MFs have been considered to be generally harmful to human health, especially in the development of leukemia and central nervous system tumors [1,2,6-9]. However, it is very difficult to protect ourselves from these low-frequency MFs, because they easily pass through human tissue and most other materials [32].

Under these conditions, there are two possible conclusions as to what can be done about MFs from dental devices:

1. Find ways to use MFs from dental devices effectively for human health promotion;
2. Abolish the devices that generate these MFs, or reduce the MF levels generated bythe dental devices.

The first conclusion was investigated and discussed in the sections above, eg. suppression of oral bacterial corrosion of intraoral dental appliances, and promotion of bone formation and repair. Further and more detailed study is needed to establish effective methods for MF utilization. With regard to the second conclusion, viable way to limit exposure to low-frequency electromagnetic fields is thought to be elimination of their generation by dental devices, eg. development of dental devices with low MF generation and keeping the devices away from tooth and metallic appliances as possible, and/or elimination of metallic appliances from oral cavity. New regulatory standards specific to human health, and particularly for the craniocervical region, are also needed in conjunction with the current conventional EMC (electromagnetic compatibility) standards, such as ISO standards.

In conclusion, further study is required to clarify the mechanisms by which the electric currents that are induced by MFs affect human oral health and to explore whether countermeasures can be developed to provide methods of protection from or methods for effective use of these effects.

Citation: Kameda T, Ohkuma K (2014) Electromagnetic Fields from Dental Devices and their Effects on Human Health. J Electr Electron Syst 3: 118. doi:10.4172/2332-0796.1000118

Page 6 of 6

Acknowledgement

The authors would like to thank Assistant Prof. Hirotake Oda (Department of Periodontology, Nippon Dental University, Niigata) for his technical assistance with bacterial cultures, and Prof. Soh Sato (Department of Periodontology, Nippon Dental University, Niigata) and Prof. Kazuto Terada (Department of Orthodontics, Nippon Dental University, Niigata) for providing valuable advice.

References

1. Ahlbom A, Day N, Feychting M, Roman E, Skinner J, et al. (2000) A pooled analysis of magnetic fields and childhood leukaemia. Br J Cancer 83: 692-698.
2. Floderus B, Persson T, Stenlund C, Wennberg A, Öst Å, et al. (1993) Occupational exposure to electromagnetic fields in relation to leukemia and brain tumors: a case-control study in Sweden. Cancer Causes Control 4: 465-476.
3. International Agency for Research on Cancer (2002) IARC monographs on the evaluation of carcinogenic risks to humans, 80 pt1.
4. International Commission on Non-Ionizing Radiation Protection (1998) Guide lines for exposure to time-varying electric, magnetic, and electromagnetic fields (up to 300 GHz).
5. World Health Organization (1987) Environmental health criteria 69: Magnetic fields. Geneva, Switzerland.
6. Thériault G, Goldberg M, Miller AB, Armstrong B, Guénel P, et al. (1994) Cancer risks associated with occupational exposure to magnetic fields among electric utility workers in Ontario and Quebec, Canada, and France: 1970-1989. Am J Epidemiol 139: 550-572.
7. Savitz DA, Loomis DP (1995) Magnetic field exposure in relation to leukemia and brain cancer mortality among electric utility workers. Am J Epidemiol 141: 123-134.
8. Kheifets L, Ahlbom A, Crespi CM, Draper G, Hagihara J, et al. (2010) Pooled analysis of recent studies on magnetic fields and childhood leukaemia. Br J Cancer 103: 1128-1135.
9. Kheifets L, Ahlbom A, Crespi CM, Feychting M, Johansen C, et al. (2010) A pooled analysis of extremely low-frequency magnetic fields and childhood brain tumors. Am J Epidemiol 172: 752-761.
10. http://www.aeha.or.jp/report/
11. Seki K, Sugano N, Nanba, K, Moriya, Y, Orii, H et al. (2003) Measurement of electromagnetic waves from dental devices. Nihon Univ Dent J 77: 359-361.
12. Kanda N, Kawabe S, Ikeda T, Takeyama M (2001) Electromagnetic wave enviromental measurement in the medical facilities -The measurement example of the dental hospital, Kenchiku Zasshi 116 suppl: 505-506.
13. http://research.lifemedia.jp/2011/06/1110601_teeth.html
14. http://www.intechopen.com/books/modern-pacemakers-present-andfuture/electromagnetic-interference-of-the-pacemakers
15. Kamimura Y, Yamada Y, Akutsu T (2005) Induced current inside the human head in the vicinity of an electric shaver. EMC J 104: 61-64.
16. Kameda T, Ohkuma K, Ishii N, Sano N, Ogura H, et al. (2012) Electric toothbrushes induce electric current in fixed dental appliances by creating magnetic fields. Dent Mater J 31: 856-862.
17. Kameda T, Ohkuma K, Sano N, Ogura H, Terada K (2013) Electric current induced in teeth by electromagnetic fields from electric toothbrushes and curing lights. Orthod Waves 72: 77-85.
18. Miyakoshi J, Yamagishi N, Ohtsu S, Mohri K, Tanabe H (1996) Increase in hypoxanthine-guanine phosphoribosyl transferase gene mutation by exposure to high density 50-Hz magnetic fields. Mutat Res 349: 109-114.
19. Jahn TL (1968) A possible mechanism for the effect of electrical potentials on apatite formation in bone. Clin Orthop 56: 261-273.
20. Bassett CA, Mitchell SN, Gaston SR (1981) Treatment of ununited tibial diaphyseal fractures with pulsing electromagnetic fields. J Bone Joint Surg 63: 511-523.
21. Schulte, A, Gente, M, Pieper, K, Arends, J (1998) The electrical resistance of enamel-dentine cylinders. Influence of NaCl content in storage solutions. J Dent 26: 113-118.
22. Lide RD (1995) Handbook of Chemistry and of Physics (75th edn.). The Chemical Rubber Co, London, UK.
23. Ortiz A, Alonso JC, Haro-Poniatowski E (2006) Spray deposition and characterization of zirconium-oxide thin films. J Electron Mater 34: 150-155.
24. Yu Y-H, Ma CC, Yuen SM, Teng CC, Huang YL, et al. (2010) Morphology, electrical, and rheological properties of silane-modified silver nanowire/polymer composites. Macromol Mate Eng 295: 1017-1024.
25. Karov J, Hinberg I (2001) Galvanic corrosion of selected dental alloys. J Oral Rehabil 28: 212-219.
26. Bakhtari A, Bradley TG, Lobb WK, Berzins DW (2011) Galvanic corrosion between various combinations of orthodontic brackets and archwires. Am J Orthod Dentofacial Orthop 140: 25-31.
27. Nagatsuma T (2002) Geomagnetic storms. J Commun Res Lab, 48: 123-136.
28. Fujii T (2011) Metal corrosion (1st edn.). Business & Technology Daily News Inc., P64.
29. Kameda T, Ohkuma K, Oda H, Sano N, Batbayar N, et al. (2013) Magnetic fields from electric toothbrushes promote corrosion in orthodontic stainless steel appliances but not in titanium appliances. Dent Mater J 32: 959-969.
30. Nash BK; Kelly RG (1993) Characterization of the crevice solution chemistry of 304 stainless steel. Corrosion Sci 35: 817-825.
31. Schiff N., Grosgogeat B, Lissac M, Dalard F (2002) Influence of fluoride content and pH on the corrosion resistance of titanium and its alloys. Biomater 23: 1995-2002.
32. http://www.cancer.gov/cancertopics/factsheet/Risk/magnetic-fields
33. Eliades T, Athanasios AE (2002) *In vivo* aging of orthodontic alloys: Implications for corrosion potential, nickel release, and biocompatibility. Angle Orthod 72: 222-237.
34. Eliades T, Bourauel C (2005) Intraoral aging of orthodontic materials: the picture we miss and its clinical relevance. Am J Orthod Dentfacial Orthop 127: 403-412.
35. Kameda T, Oda H, Ohkuma K, Sano N, Batbayar N, et al. (2014) Microbiologically influenced corrosion of orthodontic metallic appliances. Dent Mater J 33: in press.

Citation: Kameda T, Ohkuma K (2014) Electromagnetic Fields from Dental Devices and their Effects on Human Health. J Electr Electron Syst 3: 118. doi:10.4172/2332-0796.1000118

This article was originally published in a special issue, **Electromagnetic Wave Theory** handled by Editor(s). Dr. Cheng-Wei Qiu, National University of Singapore, Singapore.

Ⅲ．研究成果の刊行に関する資料⑧

J. Biomed. Mater. Res. Part B, 102B:721-728 (2014)

Society For Biomaterials

Screening study on hemolysis suppression effect of an alternative plasticizer for the development of a novel blood container made of polyvinyl chloride

Yuji Haishima,[1]* Tsuyoshi Kawakami,[2] Chie Hasegawa,[1] Akito Tanoue,[3] Toshiyasu Yuba,[4] Kazuo Isama,[2] Atsuko Matsuoka,[1] Shingo Niimi[1]

[1]Division of Medical Devices, National Institute of Health Sciences, 1-18-1 Kamiyoga, Setagaya-ku, Tokyo 158-8501, Japan
[2]Division of Environmental Chemistry, National Institute of Health Sciences, 1-18-1 Kamiyoga, Setagaya-ku, Tokyo 158-8501, Japan
[3]Department of Pharmacology, National Center for Child Health and Development, 2-10-1 Okura, Setagaya-ku, Tokyo 157-8535, Japan
[4]Corporate Research and Development Division, Kawasumi Laboratories, INC., Shinagawa Intercity Tower B, 9th Floor 2-15-2, Konan, Minato-ku, Tokyo 108-6109, Japan

Received 20 June 2013; revised 2 September 2013; accepted 22 September 2013
Published online 24 October 2013 in Wiley Online Library (wileyonlinelibrary.com). DOI: 10.1002/jbm.b.33052

Abstract: The aim of this study is to identify a plasticizer that is effective in the suppression of the autohemolysis of the stored blood and can be used to replace di(2-ethylhexyl) phthalate (DEHP) in blood containers. The results of hemolysis test using mannitol-adenine-phosphate/red cell concentrates (MAP/RCC) spiked with plasticizers included phthalate, phthalate-like, trimeliate, citrate, and adipate derivatives revealed that di-isononyl-cyclohexane-1,2-dicarboxylate (Hexamoll® DINCH), di(2-ethylhexyl)-1,2,3,6-tetrahydro-phthalate (DOTP), and diisodecyl phthalate (DIDP) exhibited a hemolysis suppression effect almost equal to that of DEHP, but not other plasticizers. This finding suggested that the presence of 2 carboxy-ester groups at the *ortho* position on a 6-membered ring of carbon atoms may be required to exhibit such an effect. The hemolytic ratios of MAP/RCC-soaked polyvinyl chloride (PVC) sheets containing DEHP or different amounts of DINCH or DOTP were reduced to 10.9%, 9.2–12.4%, and 5.2–7.8%, respectively (MAP/RCC alone, 28.2%) after 10 weeks of incubation. The amount of plasticizer eluted from the PVC sheet was 53.1, 26.1–36.5, and 78.4–150 μg/mL for DEHP, DINCH, and DOTP, respectively. PVC sheets spiked with DIDP did not suppress the hemolysis induced by MAP/RCC because of low leachability (4.8–6.0 μg/mL). These results suggested that a specific structure of the plasticizer and the concentrations of least more than ~10 μg/mL were required to suppress hemolysis due to MAP/RCC. © 2013 Wiley Periodicals, Inc. J Biomed Mater Res Part B: Appl Biomater, 102B: 721–728, 2014.

Key Words: DEHP, alternative plasticizer, hemolysis, blood container, PVC medical device

How to cite this article: Haishima Y, Kawakami T, Hasegawa C, Tanoue A, Yuba T, Isama K, Matsuoka A, Niimi S. 2014. Screening study on hemolysis suppression effect of an alternative plasticizer for the development of a novel blood container made of polyvinyl chloride. J Biomed Mater Res Part B 2014:102B:721–728.

INTRODUCTION

Phthalate esters, particularly di(2-ethylhexyl) phthalate (DEHP), have been extensively used as plasticizers due to their ability to increase the flexibility of polyvinyl chloride (PVC), a plastic polymer used in a wide array of products, including medical devices such as tubing, intravenous bags, blood containers, and catheters. DEHP is easily eluted from PVC products into food, pharmaceuticals, and body fluids that touch the plastic, causing the migration of DEHP directly and/or indirectly into the human body.[1,2]

Some phthalates, including DEHP, are considered toxic because they exhibit effects in young rodents that are similar to the antiandrogenic effects of endocrine disruptors in male rats, wherein alterations in the development of the male reproductive system and production of normal sperm are observed.[3–5] Mono(2-ethylhexyl) phthalate (MEHP) is an active metabolite of DEHP and suggested that the toxic effects of orally ingested DEHP are likely caused by the corresponding monoester, and not by the intact DEHP.[6–9] Although the *in vivo* reproductive and developmental toxicity of DEHP in the human body are not yet well understood, recent *in vitro* toxicological studies using human cells have reported that MEHP causes adverse effects such as reduction in the number of germ cells by increasing their apoptosis without altering their proliferation.[10–12] Therefore, precautions should be taken to limit human exposure to MEHP, particularly in the case of high-risk patients such as male neonates, male fetuses, and peripubertal male individuals.

The use of plasticizers other than DEHP is an option for developing safer PVC products for human use. PVC medical devices that use trioctyl trimellitate (TOTM), di-isononyl-cyclohexane-1,2-dicarboxylate (Hexamoll® DINCH),[13,14] or acetyl tributyl citrate (ATBC) instead of DEHP have already been developed and are commercially available. Several agencies and official organizations worldwide have individually evaluated the safety of DEHP released from PVC products. Recently, regulation of the use of DEHP has been tightened worldwide, particularly in Europe, not only for toys, childcare products, food apparatus, containers, and packages but also for medical devices. In many countries, including USA, Canada, and Japan, the use of alternative plasticizers to develop safer PVC products and a switch to other plastic products have been recommended for the medical treatment of high-risk patients. However, the use of PVC blood bags containing DEHP has been permitted in Japan without any regulation other than storage at low temperatures because DEHP has been found to be effective in preserving stored red blood cells (RBCs).[15]

We recently developed a prototype of a novel and biologically safer blood container consisting of UV-irradiated PVC sheets[16] from which the elution of DEHP was almost suppressed. On evaluating the safety of the prototype, we found that the hemolytic ratio of the heparinized bovine blood stocked in the container was lower than that of the blood stored in normal PVC blood bags (data not shown). It has also been reported that under periodic mixing conditions, DINCH-PVC bags exhibit protective effects against RBC hemolysis almost identical to that of normal DEHP-PVC containers.[17] These findings suggested that the ability of DEHP to prevent hemolysis must be reviewed and that some plasticizers other than DEHP may also suppress hemolysis. In the present study, we estimated the ability of multiple plasticizers to suppress hemolysis and examined the relationship between the degree of the prevention effect and the amount of plasticizer eluted from the PVC sheets as a preliminary screening in order to identify a candidate for the replacement of DEHP in RBC storage bags.

MATERIALS AND METHODS

Materials, chemicals, and utensils

Eight kinds of plasticizers were used in this study (Figure 1). TOTM, ATBC, diisodecyl phthalate (DIDP), di(2-ethylhexyl)-1,2,3,6-tetrahydro-phthalate (DOTP), bis(2-ethylhexyl) terephthalate (DEHTP), di(2-ethylhexyl) adipate (DEHA), and epoxidized soybean oil (ESBO) were purchased from Tokyo Chemical Industry Co. Ltd. (Tokyo, Japan). Hexamoll® DINCH was provided by BASF (Ludwigshafen, Germany). DEHP, DEHP-d_4, diethyl ether of pesticide residue and PCB analysis grade, and phthalate-analytical-grade hexane were purchased from Kanto Chemical (Tokyo, Japan). Sodium chloride of pesticide residue and PCB analysis grade and phthalate-analytical-grade anhydrous sodium sulfate were purchased from Wako Pure Chemical Industries, (Tokyo, Japan) and ultrapure water obtained using Milli-Q Synthesis A10 (Millipore, Tokyo, Japan) were used to prepare the sample for gas chromatography/tandem mass spectroscopy (GC-MS/MS) analysis. Heparin sodium was purchased from the Society of Japanese Pharmacopoeia (Tokyo, Japan), and other chemicals were purchased from Wako Pure Chemical Industries. All the utensils made of glass, metal, or Teflon® were heated at 250°C for more than 16 h prior to use.

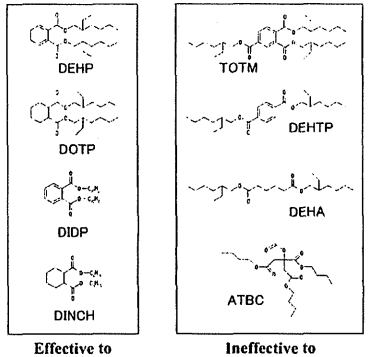

FIGURE 1. Chemical structures of the plasticizers used in this study. The iso-nonyl side-chain of DINCH consists of ~10% *n*-nonyl, 35–40% methyloctyl, 40–45% dimethylheptyl, and 5–10% methylethylhexyl isoforms. DIDP contains an isometric mixture of phthalates with primary C10 branched dialkyl chains.

Preparation of heparinized blood and MAP/RCC

Human blood (total of 200 mL) was obtained from a volunteer at our own laboratory. The procedure was performed in accordance with the ethical guidelines of the National Institute of Health Sciences (approval number 188). The blood was immediately mixed at 4°C with heparin (2000 units) or citrate-phosphate-dextrose (CPD) solution (28 mL) consisting of sodium citrate hydrate (26.3 g/L), citric acid hydrate (3.27 g/L), glucose (23.2 g/L), and sodium dihydrogen phosphate (2.51 g/L). The heparinized blood (Htc, 43%) was stocked at 4°C until use. The blood mixed with the CPD solution was centrifuged at 3000*g* for 10 min at 4°C followed by removal of the upper layer. Mannitol-adenine-phosphate (MAP) solution (46 mL) consisting of D-mannitol (14.57 g/L), adenine (0.14 g/L), sodium dihydrogen phosphate (0.94 g/L), sodium citrate hydrate (1.5 g/L), citric acid hydrate (0.2 g/L), glucose (7.21 g/L), and sodium chloride (4.97 g/L) was added to the remaining RCC layer to prepare MAP/RCC (Htc, 59%), and the solution was stocked at 4°C until use.

Correspondence to: Y. Haishima (e-mail: haishima@nihs.go.jp)

Preparation of PVC sheets

The PVC powder (100 g) was gradually added to the mixture of DEHP (55 g) and ESBO (8 g) while stirring with a spatula. The mixed powder was gently heated from room temperature to 100°C in an oven and then stirred well. The powder was stirred a second time after heating at 100°C for 5 min to completely plasticize PVC. The plasticized powder was heat-pressed at 180°C to prepare the PVC sheets (thickness = 0.4 mm; final DEHP concentration = 33.7 w/w%). The PVC powder was also plasticized in the presence of TOTM (85 g; final concentration = 44.0 w/w%), different amounts of DINCH, DIDP, or DOTP (35, 60, 85, and 110 g, respectively; final concentration = 24.5, 35.7, 44.0, and 50.5 w/w%, respectively), instead of DEHP, and then heat-pressed using the same method. Each sheet was cut into small pieces (3.2 × 1 cm).

Hemolysis test

Each plasticizer was dissolved in suitable amounts of diethyl ether, which was placed into a screw-capped glass bottle. After drying on a clean bench overnight without the bottle cap, 5 mL of heparinized blood or MAP/RCC freshly prepared was added to the bottle (final concentration: 1 or 100 μg/mL, respectively). Additionally, each PVC sheet (3.2 × 1 cm, thickness = 0.4 mm) containing different kinds and amounts of plasticizers was placed into a screw-capped glass bottle, and 5 mL of freshly prepared MAP/RCC was added to the bottle.

During incubation at 4°C for 35 days in the case of heparinized blood or 10 weeks in the case of MAP/RCC under continuous gentle shaking, an aliquot (50 μL) of the blood sample was collected into Eppendorf tubes every week. PBS (1 mL) was added to each sample and gently mixed, followed by centrifugation at 500 × *g* for 2 min at 4°C, and then the absorbance of the supernatant (100 μL) was measured at 415 nm with a SH-9000 Lab microplate reader (Corona Electric, Ibaraki, Japan). Heparinized blood or MAP/RCC alone was also tested under the same conditions as the negative control, while the positive control was prepared by adding distilled water instead of PBS. This test was repeated in triplicate, and the significant difference was calculated by two-way analysis of variance (ANOVA). The hemolytic ratio was calculated in accordance with the following formula.

$$\% \text{ Hemolysis} = (A_T - A_N)/(A_P - A_N) \times 100$$

A_T: Test sample absorbance, A_N: Average negative control mean absorbance, A_P: Average positive control mean absorbance

Elution test for the plasticizer

The quantity of plasticizer in each PVC sheet soaked with the blood samples was measured according to a previously reported method.[18-20] Briefly, an aliquot (50 μL) of MAP/RCC sample for the hemolysis test was collected into a screw-capped glass tube every week, and sodium chloride (1 mL, 1 w/v%), DEHP-d_4 (0.1 μg), and hexane (1 mL) were added. After shaking vigorously for 15 min and centrifuging at 3000 rpm for 10 min at room temperature, the organic phase was collected and dehydrated with anhydrous sodium sulfate and this was followed by GC-MS/MS analysis, as described below. This test was repeated in triplicate, concomitantly with the hemolysis test. The significant difference was calculated by two-way ANOVA.

GC-MS/MS analysis

The plasticizers in each sample were measured by GC-MS/MS, using a Trace GC with a Quantum XLS (Thermo Fisher Scientific, Waltham, MA) equipped with DB-5MS fused silica capillary column (length: 30 m, internal diameter: 0.25 mm, film thickness: 0.25 μm; Agilent Santa Clara, CA). The carrier gas was He with a flow rate of 1.0 mL/min. The temperature of the injector, transfer line, and ion source were 250°C. The sample (1 μL) was injected in the splitless mode. The GC oven temperature was initially maintained at 60°C for 2 min, and it was increased to 310°C at a rate of 20°C/min. The MS/MS system was operated under the multiple reaction-monitoring mode (MRM) with electron impact ionization (EI: 70 eV). Ar gas was used as the collision gas (0.13 Pa). The retention times, the precursor (Q1) and product (Q2) ions of the plasticizers, and the collision energies of each plasticizer were listed in Table I.

The product ions of all the plasticizers were used for quantification that was performed using DEHP-d_4 as the internal standard. The concentrations of DINCH and DIDP were determined using the sum of the total peak area of their isomers, similar to a previous study.[21] The limits of detection and quantification (LOD and LOQ, respectively) were calculated using total optimization of chemical operations (TOCO) software version 2.0 and the function of mutual information (FUMI) theory.[22] The concentrations obtained using the relative standard deviations of 33% and 10% on the basis of the mass chromatograms of the standard and blank solutions, respectively, were used as the instrumental LOD and LOQ. The recovery test was conducted by adding every compound to the blood sample (10μg/mL, n=5). The blank test was conducted using the blood sample without PVC sheets. Only DEHP was detected under the LOQ level.

TABLE I. Retention Times, Precursor Ions (Q_1), Product Ions (Q_2), Collision Energies, LODs, LOQs, Recoveries, and its Coefficients of Variation (CV) of the Target Chemicals.

Chemicals	Retention Time (min)	Q_1 (m/z)	Q_2 (m/z)	Collision Energy (V)	LOD[a] (ng/mL)	LOQ[a] (ng/mL)	Recovery[b] (%)	CV (%)
DOTP	14.34	170	124	7	0.12	0.39	101	2.8
DEHP	14.54	167	149	4	0.051	0.17	99	1.5
DINCH	14.60-16.60	155	109	5	0.45	1.5	101	1.8
DIDP	15.60-17.60	307	149	13	0.64	2.1	109	5.5
TOTM	20.97	305	193	16	0.040	0.13	123	7.1
DEHP-d_4[c]	14.53	171	153	4				

[a] Calculated by TOCO version 2.0 (FUMI theory). The values correspond to the concentration in the injected solution.
[b] Adding every compound to the blood sample (10 μg/mL, n = 5).
[c] Internal standard.

RESULTS

Identification of an alternative plasticizer effective in suppressing hemolysis

First, we estimated whether the plasticizer itself exhibited the suppression effect on hemolysis. As shown in Figure 2, the hemolytic ratio of the heparinized blood in the absence of plasticizers increased in a time-dependent manner and reached 61.6% after 35 days of incubation (control). The hemolysis behavior of the heparinized blood spiked with each plasticizer was similar to that of the control or was slightly higher, indicating that all the plasticizers were ineffective in suppressing hemolysis irrespective of the type and amount spiked. Although all the plasticizers did not exhibit hemolysis suppression against MAP/RCC at the concentration of 1 μg/mL [Figures 3(a,b)], the hemolytic ratio of MAP/RCC spiked with DINCH, DIDP, or DOTP at the dose of 100 μg/mL significantly decreased to 10.3%, 12.1%, and 9.5%, respectively, in comparison with the ratio of MAP/RCC containing no additives, which reached 18.9% after 10 weeks of incubation [Figure 3(c)]. The degree of the effect of the plasticizers was almost identical to that of DEHP (hemolysis ratio = 10.9% after 10 weeks of incubation). Additionally, TOTM, ATBC, DEHTP, and DEHA did not suppress the hemolysis of MAP/RCC even at the concentration of 100 μg/mL [Figure 3(d)].

Hemolysis suppression by the PVC sheet containing plasticizer

Similar to the result of the first screening, PVC sheets spiked with different amounts of DINCH, DIDP, or DOTP were prepared, and their hemolysis suppression effect against MAP/RCC was estimated. The size of the PVC sheet and the amount of MAP/RCC used in this study were decided based on the ratio between the inner surface area and the blood volume of the typical RBC storage bags (KARMI Blood Bag KBQ-200AML, Kawasumi Laboratories, INC., Tokyo, Japan). The PVC sheets spiked with DEHP or TOTM were used as the positive or negative control, respectively.

As shown in Figure 4(a), the hemolytic ratio of MAP/RCC in the absence of the PVC sheets increased in a time-dependent manner and reached 29.4% after 10 weeks of

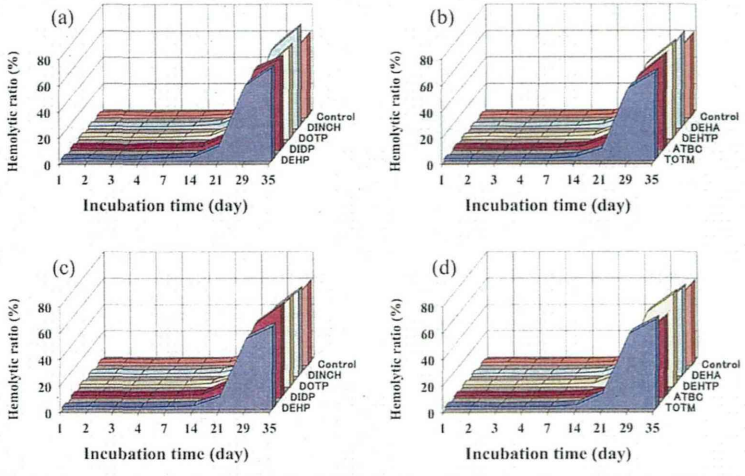

FIGURE 2. Hemolytic behavior of heparinized blood containing plasticizers at the concentration of 1 μg/mL (a, b) or 100 μg/mL (c, d). No significant difference was detected between the control and each plasticizer irrespective of the type and amount spiked. [Color figure can be viewed in the online issue, which is available at wileyonlinelibrary.com.]